In search of Global 21 cm signal using Artificial Neural Network in light of EDGES and ARCADE 2

Pravin Natwariya

Theoretical Physics Division,
Physical Research Laboratory, India.

Bled Workshop
July 15, 2023

21 cm signal

- The 21 cm signal appears to be a treasure trove to study physics during cosmic dawn and reionization.
- The 21 cm line has been actively used to trace the neutral hydrogen in Milky Way for more than seven decades.

21 cm signal

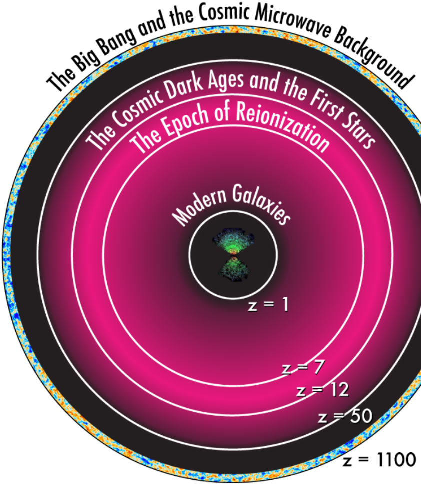

Dillon (2015) arXiv:1506.03024; originally reproduced from Tegmark & Zaldarriaga (2009)

- Differential brightness temperature:

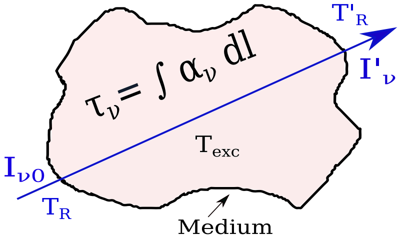

$$\delta T_B = T'_{\rm R} - T_{\rm R}$$

$$\frac{dI_\nu}{dl} = j_\nu - \alpha_\nu I_\nu \xrightarrow[\mathcal{I}_\nu = 2\nu^2 T]{2\pi\nu/T \ll 1} T'_{\rm R} = T_{\rm exc}\,(1 - e^{-\tau_\nu}) + T_{\rm R}\, e^{-\tau_\nu}\ .$$

$$\delta T_B = (T_{\rm exc} - T_{\rm R})(1 - e^{-\tau_\nu})$$

What is the 21 cm signal?

- For the 21 cm line: $T_{\mathrm{exc}} = T_S$ (spin temperature),

- characterised by number density ratio in the hyperfine states,
  - $\frac{n_{\mathrm{T}}}{n_{\mathrm{S}}} = \frac{g_{\mathrm{T}}}{g_{\mathrm{S}}} \times \exp\left[-\frac{2\pi\nu_{\mathrm{TS}}}{T_S}\right]$, $\nu_{\mathrm{TS}} = 1420\ \mathrm{MHz} = 1/(21\ \mathrm{cm})$

- For neutral hydrogen medium (expanding Universe),

What is the 21 cm signal?

- For the 21 cm line: $T_{\rm exc} = T_S$ (spin temperature),

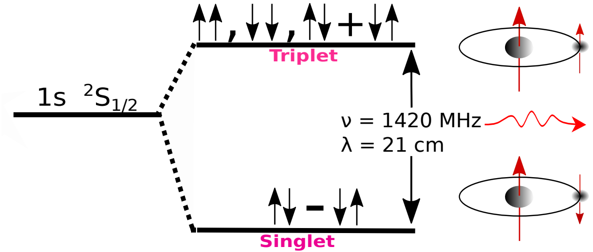

- characterised by number density ratio in the hyperfine states,
  - $\frac{n_{\rm T}}{n_{\rm S}} = \frac{g_{\rm T}}{g_{\rm S}} \times \exp\left[-\frac{2\pi\nu_{\rm TS}}{T_S}\right]$, $\nu_{\rm TS} = 1420\ {\rm MHz} = 1/(21\ {\rm cm})$

- For neutral hydrogen medium (expanding Universe),

What is the 21 cm signal?

- For the 21 cm line: $T_{\mathrm{exc}} = T_S$ (spin temperature),
- characterised by number density ratio in the hyperfine states,
  - $\frac{n_{\mathrm{T}}}{n_{\mathrm{S}}} = \frac{g_{\mathrm{T}}}{g_{\mathrm{S}}} \times \exp\left[-\frac{2\pi\nu_{\mathrm{TS}}}{T_S}\right]$, $\nu_{\mathrm{TS}} = 1420\ \mathrm{MHz} = 1/(21\ \mathrm{cm})$
- For neutral hydrogen medium (expanding Universe),

$$\boxed{\delta T_B \;=\; T_{21} = \frac{T_{\mathrm{S}} - T_{\mathrm{R}}}{1+z}(1 - e^{-\tau_\nu}), \quad \tau_\nu \approx \frac{3\,A_{10}\,n_{\mathrm{HI}}}{16\nu_{\mathrm{TS}}^2\,H\,T_{\mathrm{S}}}}$$

21 cm signal and its evolution

- Absorption/emission in 21 cm line: $T_{21} \propto (1 - T_R/T_S)$.
- Below $z \sim 200$ (ΛCDM): $T_{\mathrm{gas}} \propto (1+z)^2$, $T_{\mathrm{CMB}} \propto (1+z)$.

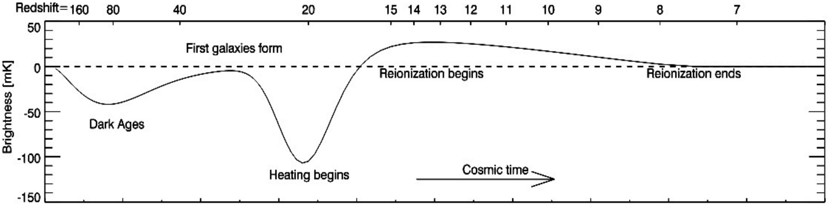

Pritchard & Loeb, Rep. Prog. Phys. 75, 086901 (2012)

EDGES low band observation

- In 2018, such an absorption at $z \sim 17$ has been confirmed by EDGES observation:

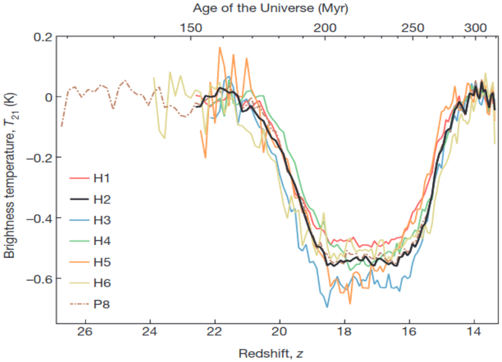

Bowman et al. 2018, Nature, 555, 67

EDGES low band observation

- It is centered at 78 ± 1 MHz or $z = 17.2 \pm 0.2$. Here, $\nu_0 = \frac{\nu}{1+z}$ and $\nu = 1420$ MHz.
- To explain the EDGES anomaly, one requires to enhance T_{R} (Radio Background) above T_{CMB} or lower T_{gas} below 3.2 K at redshift ~ 17.

Observations of Excess Radio Background

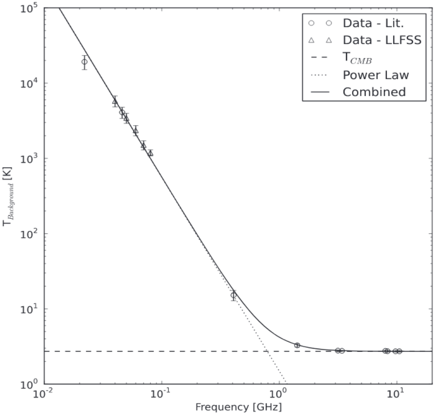

ARCADE2 (2011) [Fixsen et al., APJ, 11]; LWA1 (2018) [Dowell et al., APJL, 18]

Observations of Excess Radio Background

- ARCADE 2 observed Excess: 3-10 GHz
  - Combining ARCADE 2 with other Low-frequency data gives excess in the range of 22 MHz—10 GHz.
- Also supported by LWA-1 in range: 40-80 MHz.
- This excess radio radiation can also explain the EDGES anomaly.
- There are several theoretical models to explain this excess at CD, for e.g., axion-photon conversion & synchrotron radiation from electron in the presence of IGM MFs, radiative decays of relic neutrinos, accretion onto the first intermediate-mass BHs, etc.
- The excess radiation can be modelled as:[1]

$$T_R = T_{\rm CMB}\,(1+z)\,\left[1 + A_r\,\left(\frac{\nu_{\rm obs}}{78\ {\rm MHz}}\right)^{\beta}\,\right],$$

[1]Fialkov & Barkana, MNRAS 486, 1763 (2019)

IGM in the presence of Excess Radio and X-ray heating

- IGM gas temperature evolution:

$$\frac{dT_{\rm gas}}{dz} = 2\,\frac{T_{\rm gas}}{1+z} + \frac{\Gamma_c}{(1+z)\,H}(T_{\rm gas} - T_{\rm CMB})$$

- Inclusion of first stars effect[2]:

$$+\frac{dT_{\rm gas}}{dz}\bigg|_{\rm x-ray} - \frac{\Gamma_R}{(1+z)\,(1+f_{He}+X_e)};\ \Gamma_R = X_{\rm HI}\,\frac{A_{10}}{2\,H}\,x_R\left[\frac{T_R}{T_S}-1\right]\,T_{10}\,.$$

[2] Venumadhav et al., PRD 98, 103513 (2018).

IGM gas temperature evolution for different cases

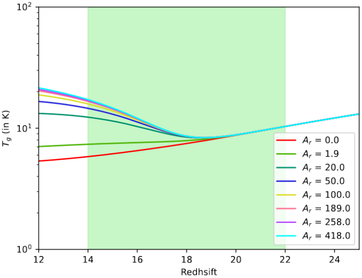

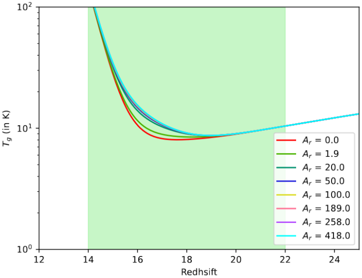

- Increases excess radiation fraction (A_r) above 100, does not significantly change the $T_{\rm gas}$.
- Because $\Gamma_R \propto (T_R/T_S - 1) \sim T_R/T_S$
- Coupling between $T_{\rm gas}$ and T_S are $\propto 1/T_R$.

Global 21 cm signal for different cases

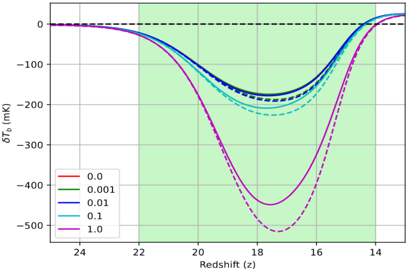

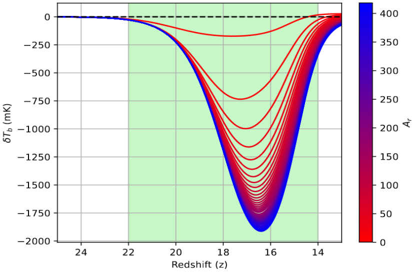

Free parameters related to IGM temperature & Ly-α coupling

$$\mathrm{x}_{\alpha} = \mathrm{x}_{\mathrm{ref}} \left(1 + \tanh\left\{\left(x_{z0} - z\right) / x_{dz}\right\}\right)$$

$$\mathrm{T}_{\mathrm{xray}} = \mathrm{T}_{\mathrm{ref}} \left(1 + \tanh\left\{\left(T_{z0} - z\right) / T_{dz}\right\}\right)$$

Foreground model considered for EDGES signal

$$T_{\mathrm{FG}}(\nu) \approx \left(\frac{\nu}{\nu_0}\right)^{-2.5} [b_0 + b_1 \ln(\nu/\nu_0) + b_2(\ln(\nu/\nu_0))^2 + b_3(\nu/\nu_0)^{-2} + b_4(\nu/\nu_0)^{0.5}]\mathrm{K}$$

21 cm data for machine training

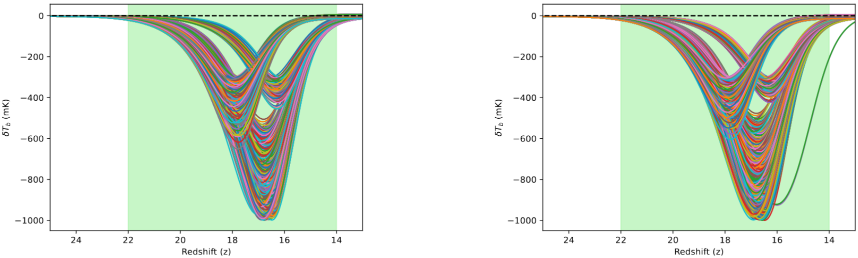

Inclusion of foreground

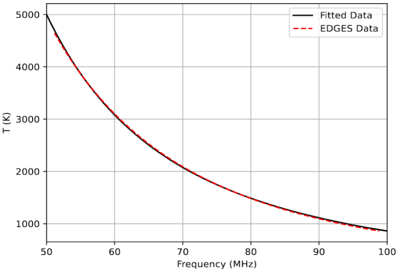

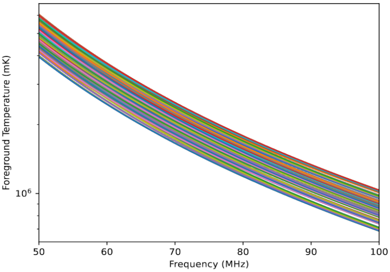

Pearson correlation in IGM parameters

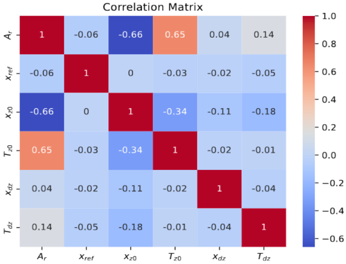

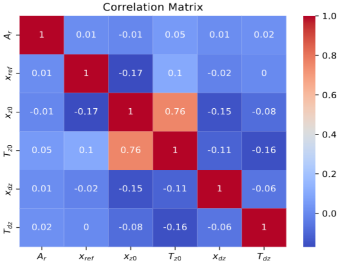

Pearson correlation in FG parameters

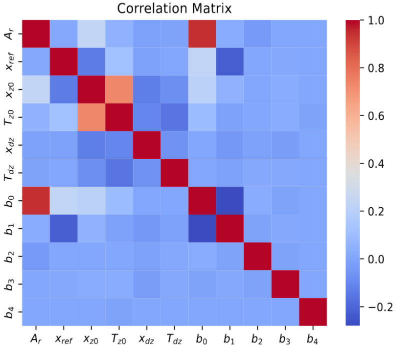

Prediction of parameters with RMSE and R2 score

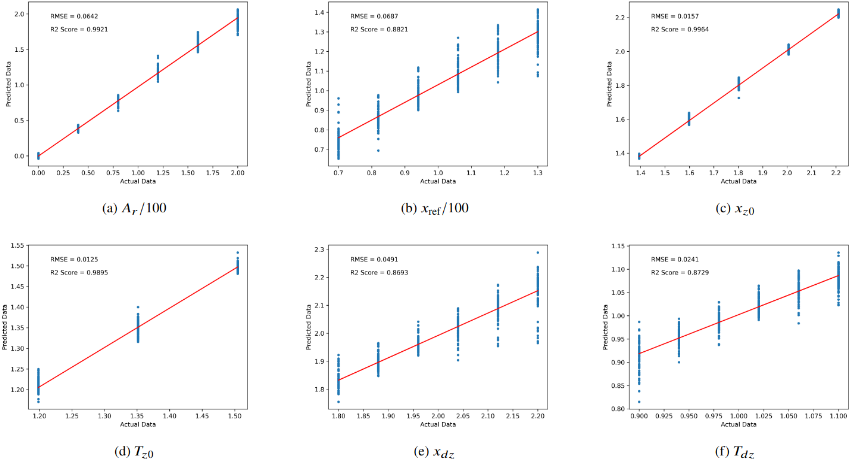

Figure 11. Each plot above shows the prediction of the aforementioned parameters with RMSE and R2 score assigned in the absence of the VDKZ18.

Loss while training

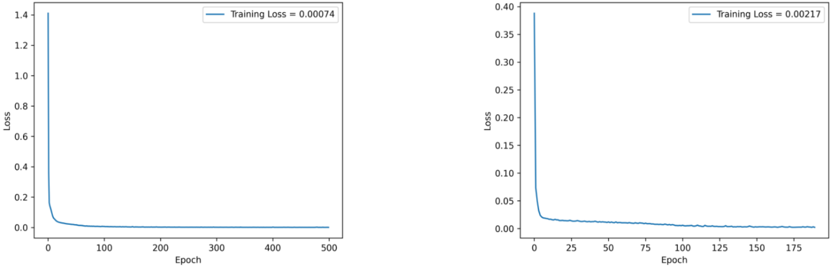

(a) (b)

Figure 9. Variation of the model loss during the training process, where (a) in the presence of the VDKZ18 and (b) in the absence of the VDKZ18

Model loss & prediction of parameters with RMSE and R2 score

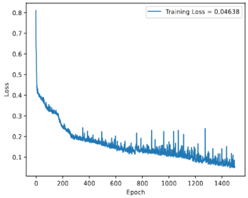

(a) Model Loss with epoch

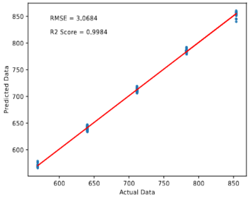

(b) b_0

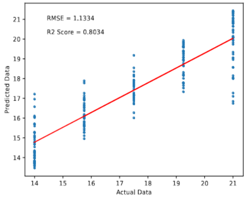

(c) b_1

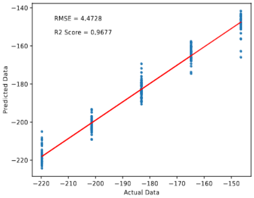

(d) b_2

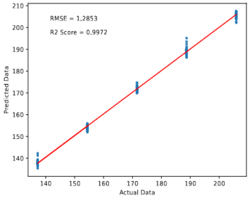

(e) b_3

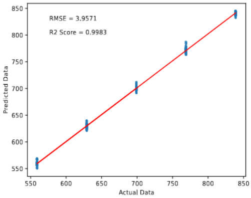

(f) b_4

Summary & conclusion

Summary and conclusion

- The signal can provide a good insight into the period when the galaxies and first stars formed.
- We generated synthetic data by resolving the typical cosmological equations
- The accuracy of one of our estimations is evaluated by examining the RMSE and R2 scores for each case
- As far as our understanding goes, most authors have employed Markow Chain Monte Carlo (MCMC), nested sampling, or similar methods for parameter space sampling.
- As ANN (Artificial Neural Network) and MCMC have different methodologies, we cannot directly compare their speed.

Summary and conclusion

- However, ANN offers the advantage of bypassing the requirement of computing the likelihood function multiple times to derive inferred parameter values.
- Thus, when dealing with a higher dimensional parameter space, ANN is computationally more efficient and faster.
- In future works, we wish to include energy injection terms linking directly to the first star's astrophysical properties, instrument response and contamination model to make the NN more robust.
- Also, we intend to apply this concept and algorithm to more realistic data, like EDGES, SARAS 3, SKA, etc.

Thank You!

A brief introduction to evolution of our Universe

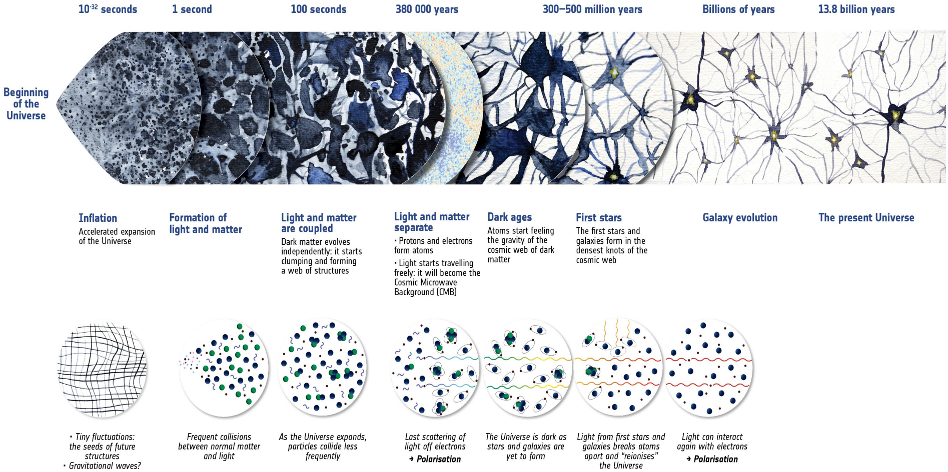

Image credits: European Space Agency (ESA)

Collisional & Lyα coupling coefficients

- The collisional coupling coefficient[3],

$$x_c = \frac{P^{\mathrm{C}}_{\mathrm{TS}}}{P^{\mathrm{R}}_{\mathrm{TS}}} = \frac{T_{10}}{T_R\, A_{10}} \times (N_H\, k_{10}^{HH} + N_e\, k_{10}^{He} + N_p\, k_{10}^{Hp}), \quad P^{\mathrm{R}}_{\mathrm{TS}} = \left(1 + \frac{T_R}{T_{10}}\right) A_{10}$$

- k_{10}^{ij} scattering rate between i & j particles
- After the inclusion of x-ray and VDKZ18 heating effects, the gas temperature remains > 10 K.
- Therefore, we can take (for $10\ \mathrm{K} < T_{\mathrm{gas}} < 10^3\ \mathrm{K}$),

$$k_{10}^{HH} \approx 3.1 \times 10^{-11} (T_{\mathrm{gas}}/\mathrm{K})^{0.357} \exp(-32\ \mathrm{K}/T_{\mathrm{gas}})\ \mathrm{cm}^3/\mathrm{sec}$$

- WF coupling coefficient: $x_\alpha = T_{10}/(T_R\, A_{10}) \times 4P_\alpha/27$, P_α scattering rate of Lyα photons[4]. Einstein coefficient: $A_{10} = 2.85 \times 10^{-15}\ \mathrm{sec}^{-1}$

[3] Pritchard & Loeb, Rep. Prog. Phys. 75, 086901 (2012)
[4] Wouthuysen S. A., ApJ, 57, 31 (1952). Field G. B., Proc. IRE, 46, 240 (1958).

Collisional & Lyα coupling coefficients

- WF coupling[5]:

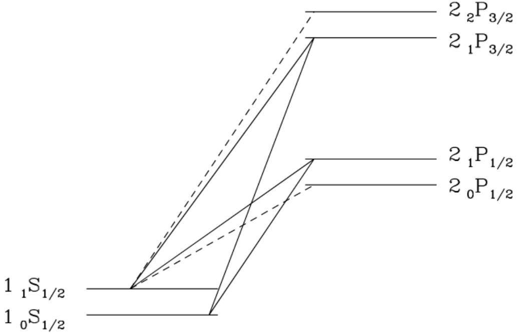

- we consider $x_\alpha = 2A_\alpha(z) \times (T_0/T_R)$, step height $A_\alpha = 100$, pivot redshift $z_{\alpha 0} = 17$ & $\Delta z_\alpha = 2$, $A_i(z) = A_i(1 + \tanh[(z_{i0} - z)/\Delta z_i])$. [6]
- $\{A_X, z_{X0}, \Delta z_X\} = \{1000\ \mathrm{K},\ 12.75,\ 1\}$, $\{A_{xe}, z_{xe}, \Delta z_{xe}\} = \{1,\ 9,\ 3\}$.

[5] Furlanetto et al., Phys. Rept. 433 (2006) 181-301.
[6] Kovetz et al., PRD 98, 103529 (2018); Mirocha et al., ApJ. 813, 11 (2015); Harker et al., MNRAS, 455, 3829 (2016).

Frequencies and wavelengths

Category	Range of Wavelengths (nm)	Range of Frequencies (Hz)
gamma rays	< 1	$> 3 \times 10^{17}$
X-rays	$1 – 10$	$3 \times 10^{16} – 3 \times 10^{17}$
ultraviolet light	$10 – 400$	$7{,}5 \times 10^{14} – 3 \times 10^{16}$
visible light	$400 – 700$	$4{,}3 \times 10^{14} – 7{,}5 \times 10^{14}$
infrared	$700 – 10^5$	$3 \times 10^{12} – 4{,}3 \times 10^{14}$
microwave	$10^5 – 10^8$	$3 \times 10^{9} – 3 \times 10^{12}$
radio waves	$> 10^8$	$< 3 \times 10^{9}$

$$\mathrm{Ly}\alpha = 2.47 \times 10^9\ \mathrm{MHz}$$

21-cm signal and spin temperature

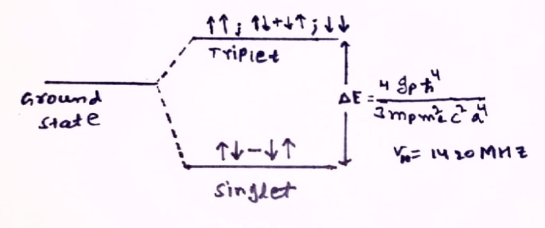

$$\frac{dn_0}{dt} = -n_0 P_{01}^c + n_1 P_{10}^c \,,$$

- P_{01}^c & P_{10}^c are excitation and deexcitation coefficients.
- In the equilibrium, $\frac{n_1}{n_0} = \frac{P_{01}^c}{P_{10}^c} \Rightarrow \frac{P_{01}^c}{P_{10}^c} = \frac{g_1}{g_0}\ \exp\left[-\frac{2\pi\nu_{10}}{T_{\rm gas}}\right]$,
- $T_S = T_{\rm gas}$ because in equilibrium T_S will reach to the $T_{\rm gas}$.
- Planck spectrum, $B_\nu(T) = \frac{2h\nu^3/c^2}{\exp(h\nu/k_b T)-1}$, in the Rayleigh–Jeans regime, $2\pi\nu/T \ll 1$, $B_\nu(T) = 2\nu^2 T$.

21-cm signal and spin temperature

$$I_\nu = S_\nu(1 - e^{-\tau}) + I_{\nu_0}\, e^{-\tau}$$

- Hydrogen is characterized by T_S, $S_\nu(T) = j_\nu/\alpha_\nu \equiv B_\nu(T_S)$. $I_{\nu_0} = B_\nu(T_{\rm CMB})$.

$$I_\nu(T_B) = I_\nu(T_S)\,(1 - e^{-\tau}) + I_\nu(T_{\rm CMB})\, e^{-\tau}\ ,$$

- T_B is final brightness temperature.
- 21 cm differential brightness temperature, $T_{21} = T_B - T_{B_0}$.
- $T_{B_0} = T_B(\tau = 0) = T_{CMB}$. $T \propto (1 + z)$. Therefore, the observed,

$$\boxed{T_{21} = \frac{T_S - T_{\rm CMB}}{1 + z} \times (1 - e^{-\tau})}.$$

- To find τ, write complete eq,

$$\frac{dI_\nu}{dl} = \frac{h\nu_e}{4\pi}\phi(\nu)[n_1 A_{10} + I_\nu n_1 B_{10} - I_\nu n_0 B_{01}].$$

Hyperfine splitting$^{(4)}$

- Dipole moments of electron and proton[7]:

$$\boldsymbol{\mu}_e = -\frac{(g_e = 2)\, e}{2\, m_e}\, \mathbf{S}_e \quad \& \quad \boldsymbol{\mu}_p = \frac{(g_p = 5.59)\, e}{2\, m_p}\, \mathbf{S}_p\,.$$

- Magnetic field due to dipole ($\boldsymbol{\mu}$):

$$\mathbf{B} = \frac{\mu_0}{4\,\pi\, r^3}[3\,(\boldsymbol{\mu}\cdot\hat{r})\,\hat{r} - \boldsymbol{\mu}] + \frac{2\,\mu_0}{3}\,\boldsymbol{\mu}\,\delta^3(\mathbf{r})\,.$$

- Hamiltonian of electron in the presence of Magnetic field due to dipole of proton:

$$H_{\mathrm{HF}} = -\boldsymbol{\mu}_e \cdot \mathbf{B}_p\,.$$

- Expectation value:

$$E_{\mathrm{HF}} = \frac{4\, g_p}{3\, m_p\, m_e^2\, a^4} \times \Big|_{-3/4}^{+1/4}$$

- Energy gas: $\Delta E = 5.88 \times 10^{-6}$ eV
- Corresponding $\nu = \Delta E/2\pi \simeq 1420.4$ MHz & $\lambda \simeq 21$ cm.

[7]Quantum Mechanics by David J. Griffiths